INTERNATIONAL JOURNAL OF PRECISION ENGINEERING AND MANUFACTURING Vol. 15, No. 11, pp. 2357-2366 NOVEMBER 2014 / 2357
DOI: 10.1007/s12541-014-0601-9

An Analyzing Method of Coupled Modes in Multi-Stage Planetary Gear System

Wei Sun[1], Xin Ding[1], Jing Wei[1,#], Xinglong Hu[1], and Qingguo Wang[1]

1 School of Mechanical Engineering, Dalian University of Technology, Dalian, P. R. China, 116-024
Corresponding Author / E-mail: weijing@dlut.edu.cn, TEL: +86-411-8470-7435, FAX: +86-411-8470-8414

KEYWORDS: Multi-stage planetary gears, Natural frequency and vibration mode, Coupling, Parameter sensitivity

This paper analyzed the natural frequency and coupled mode characteristics in multi-stage planetary gear system. A dynamic model of multi-stage planetary gears with general description is established based on the lumped mass method. Solving the associated eigenvalue problem, the vibration modes of the system with identical, equally spaced planets are classified into rotational, translational and planet modes with unique properties. A criterion to distinguish the dominant vibration stage for the two coupled mode types, rotational mode and translational mode, are provided by comparing the eigensensitivity to the component parameters of different planetary stages. Taken the dominant vibration stage as an independent single-stage planetary gear system, the natural frequencies and vibration modes are observed to be similar to the multi-stage. It is shown that the coupling in the multi-stage planetary gear system grows as the frequency reduces. In rotational modes and translational modes, the highest eigensensitivity to mesh stiffness and planet bearing stiffness of each stage are associated with different frequencies in the higher-frequency range, while the highest eigensensitivity to bearing stiffness of carriers, rings, and suns occurred in the lower-frequency range.

Manuscript received: May 8, 2014 / Revised: July 15, 2014 / Accepted: July 19, 2014

NOMENCLATURE

Λ = number of degrees of freedom
a = number of planetary stages
N^j = number of planet gears in planetary stage j
k^j_{lu} = bearing stiffness, $l = c, r, s, p$
k^j_{lu} = torsional stiffness, $l = c, r, s$
k^j_{rp}, k^j_{sp} = ring-planet and sun-planet mesh stiffness
k^{ij}_{cs}, $k^{ij}_{cs,u}$ = shaft stiffness between carrier in planet stage i and sun in planet stage j
m = mass
I = mass moment of inertia
x, y = translational coordinate
r = radius (base radius for gears, radius to planet centers for carriers)
θ = rotational coordinate
u = rotational coordinate, $u=r\theta$
ζ, η = planet radial and tangential coordinates
α^j_r, α^j_s = ring-planet and sun-planet mesh pressure angles in planet stage j
$\varphi^j_n(t)$ = angular position of planet n in planet set
e = static transmission error
$F(t)$ = externally applied force
$T(t)$ = externally applied torque
ω_i = i-th natural frequency
ϕ_i = i-th vibration mode
$\delta^{j,v}_{sn}$ = deformation of the nth sun-planet mesh of planet stage j in mode ϕ_v

1. Introduction

Planetary gears are widely used in many applications like automobiles, helicopters and tunneling boring machine (TBM) due to their advantages, such as high power density and large reduction in a small volume.[1] Given the growing requirements of higher speed and heavier load in applications, hence, the multi-stage planetary gears are commonly used due to the benefits of greater reductions and more load transmissions. Despite their benefits, the multi-stage planetary gears

often have more noise and vibration problems than single-stage planetary gears.[2]

The majority of research discussing free vibration for planetary gear has focused on simple, single stage systems. Lin and Parker[3] analytically classified all planetary gear modes into exactly three categories, rotational, translational, and planet modes, as well as their certain unique properties. Recently, the existence of three mode types was experimentally confirmed and the clustering phenomenon of the natural frequencies of planetary gears was investigated.[4] The systematic classification of modes is carried out in systems modeled with helical planetary gear trains,[5] compound planetary gears,[6] flexible ring gears and planet carriers.[7] In the research of system parameter sensitivities on planetary gear natural frequencies and modes, Lin and Parker[8] rigorously investigated the eigensensitivities to different parameters for both tuned and mistuned planetary gears. Wang[9] studied the natural frequency veering with variation in system parameters and investigated the theory of planet phasing.

Contrast to the simple, single-stage planetary gears, the vibration of the multi-stage planetary gears has attracted little research attention. Kiracofe,[10] mathematically proved that compound, multi-stage planetary gear systems of general description possess highly structured modal properties analogous to simple, single-stage planetary gears. Guo, et al[11] analyzed the sensitivity of natural frequencies and vibration modes in compound planetary gears to system parameters. Qing, et al,[12] and Wei, et al,[13] studied the nonlinear dynamic characteristics of the multi-stage planetary gears for TBM and wind turbine applications.

Generally, current research only classified the vibration modes into rotational, translational, and planet modes by considering the information about central member motions in planetary gear system. However, in multi-stage planetary gear system, there are multiple degrees of freedom, which determine the number of natural frequencies and vibration modes. Although mode type classifications above exist, it is difficult to generalize characteristics in each mode only by visual inspection. The objective of this paper is to propose a novel method of analyzing coupled modes in multi-stage planetary gears. Using the modal properties and eigensensitivity calculation, simple criterions to distinguish dominant vibration stage for each mode type are provided. Knowledge of the natural frequency and vibration characteristics provides more guidance for tuning natural frequencies to avoid powertrain resonances.

2. Modeling and Equations of Motion

2.1 Coordinates and geometric description

The multi-stage planetary gears are created by joining multiple planetary stages together, where each stage can be a simple planetary. Fig. 1 shows a three-stage planetary gear system used in the driving system of TBM.[14]

A lumped-parameter model for multi-stage spur planetary gears is shown in Fig. 2.[15] In each stage, all the sun, ring, carrier and planets are treated as rigid bodies. Component bearings are represented as linear springs between the bodies and their housings. Gear mesh interactions are represented by linear springs acting along the line of action. Each component has three degrees of freedom: two translations and one

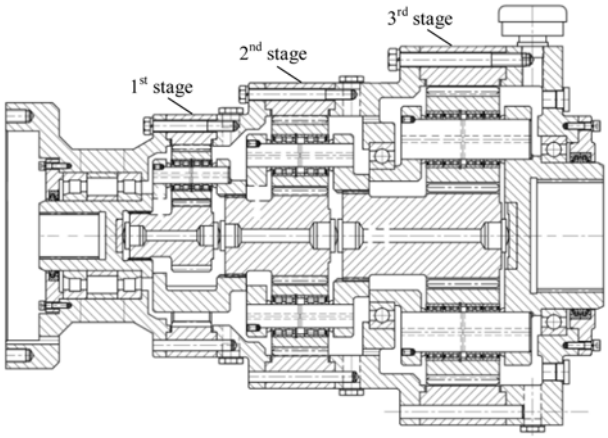

Fig. 1 One three-stage planetary gear system for TBM

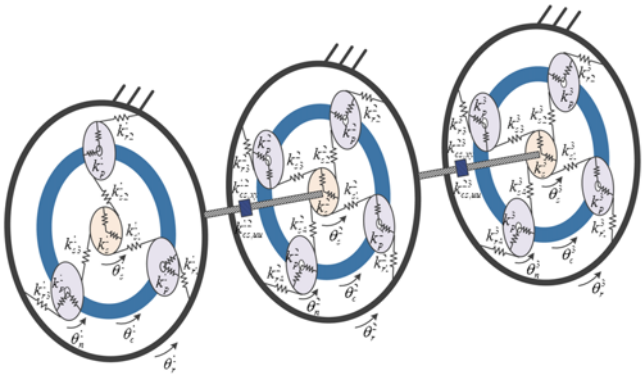

Fig. 2 Mathematics model of multi-stage planetary gear system

rotation. Coupling between two adjacent stages is represented as one torsional stiffness and two directions of translation coupling stiffness. In total, the degrees of freedom Λ in the model is

$$\Lambda = 3\left(3a + \sum_{j=1}^{a} N^j\right) \tag{1}$$

Where a is the quantity of planetary stages, j is the number of one arbitrary planetary stage, and N^j denotes the quantity of planet gears in planetary stage j. For convenient enumeration, carrier j, sun j and ring j associated with the planetary stage j are also used in this paper.

In the model, all components of each planetary stage are described in a single fixed basis, and the planet position angles in each stage change with time. Fig. 3 shows the equivalent dynamics model of single-stage planetary gears and coordinates.[16] Translational coordinates x_l^j, y_l^j, $l = c, r, s$ are assigned to the carriers and the central gears (rings and suns). The x_l^j, $l = c, r, s$ coordinates are directed towards the equilibrium position of the arbitrarily chosen first planet at time t=0. Translational coordinates ζ_n^j, η_n^j are assigned to planet n, standing for absolute radial and tangential deflections of the n-th planet gear respectively. The origin of ζ_n^j, η_n^j coordinates is fixed at each planet's equilibrium position and does not translate with carrier vibration. The rotational coordinates are $u_l^j = r_l^j \theta_l^j$, $l = c, r, s, 1, \ldots, N^j$; where θ_l^j is the component rotation; r_l^j is the base circle radius for the sun j, ring j and planet j, and the radius of the carriers is measured by the radius from

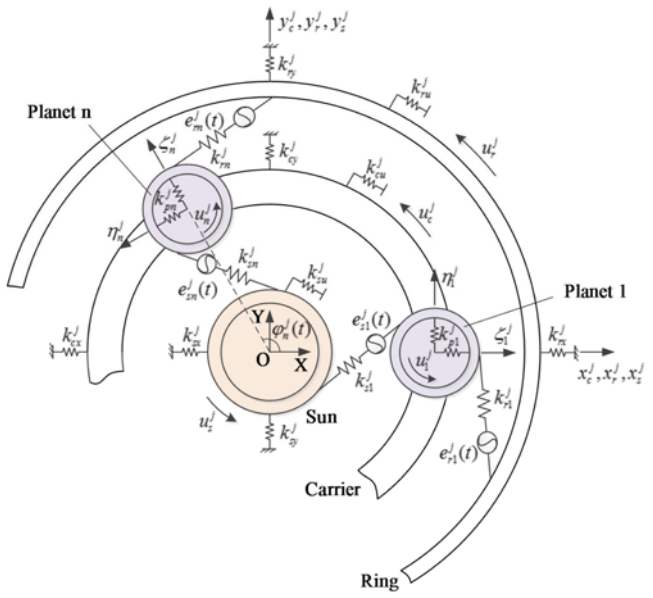

Fig. 3 Equivalent dynamics model of planetary stage j

the carrier center to the planet center. The circumferential planet locations are specified by the time varying angles $\varphi_n^j(t)$, where $\varphi_1^j(0)=0$. This angle is measured clockwise from the positive ζ direction of planet n to the line connecting the centers of arbitrarily chosen first planet and the origin O.

2.2 Equations of motion

The equations of motion of a sun gear are derived as an example. The deflection of the n-th sun-planet mesh in planetary stage j[17] is

$$\begin{aligned}\delta_{sn}^j = u_s^j + u_n^j - x_s^j \sin\psi_{sn}^j(t) + y_s^j \cos\psi_{sn}^j(t) \\ -\zeta_n^j \sin\alpha_s^j - \eta_n^j \cos\alpha_s^j + e_{sn}^j(t)\end{aligned} \tag{2}$$

Where α_s^j is the pressure angle of the sun-planet mesh, and $\psi_{sn}^j(t) = \varphi_n^j - \alpha_s^j + \omega_c^j t$, ω_c^j is the angular velocity of the carrier in j-th stage. $e_{sn}^j(t)$ is the time-varying, unloaded static transmission error.

The coupling interaction between the sun j and the carrier i in x direction is described as $k_{cs,xy}^{ij}(x_s^j - x_c^i)$, which is the same for the y and u coordinates. The equations of motion[17] for the sun in stage j are

$$\begin{cases} m_s^j \ddot{x}_s^j + k_{sx}^j x_s^j - \sum_{n=1}^{N^j} k_{sn}^j \delta_{sn}^j \sin\psi_{sn}^j(t) + \sum_{i=1}^{a} k_{cs,xy}^{ij}(x_s^i - x_c^i) = F_x^j(t) \\ m_s^j \ddot{y}_s^j + k_{sy}^j y_s^j - \sum_{n=1}^{N^j} k_{sn}^j \delta_{sn}^j \cos\psi_{sn}^j(t) + \sum_{i=1}^{a} k_{cs,xy}^{ij}(y_s^j - y_c^i) = F_y^j(t) \\ \dfrac{I_s^j}{(r_s^j)^2}\ddot{u}_s^j + k_{su}^j u_s^j - \sum_{n=1}^{N^j} k_{sn}^j \delta_{sn}^j + \sum_{i=1}^{a} \dfrac{k_{cs,u}^{ij}}{r_s^j}\left(\dfrac{u_s^j}{r_s^j} - \dfrac{u_c^i}{r_c^i}\right) = \dfrac{T_s^j(t)}{r_s^j} \end{cases} \tag{3}$$

The equations of motion for the rings, carriers and planets are obtained similarly. The matrix form of system equations is

$$M\ddot{q}(t) + [K_b + K_m(t)]q(t) = F(t) \tag{4}$$

Where **M** is the mass matrix, K_b is the bearing stiffness matrix, $K_m(t)$ is the symmetric stiffness matrix from both tooth meshes and shaft couplings, and $F(t)$ is the vector of applied forces and torques.

Table 1 Parameters of the example system

Parameter	Parameter Values
Number of Stages	a=3
Planet Number	N^1=3, N^2=N^3=4
Pressure Angle	$\alpha_r^1 = 21.7°$, $\alpha_r^2 = 21.3°$, $\alpha_r^3 = 21.1°$ $\alpha_s^1 = 21.7°$, $\alpha_s^2 = 21.3°$, $\alpha_s^3 = 21.1°$
Mass (kg)	$m_c^1 = 17.7$, $m_r^1 = 30.7$, $m_s^1 = 4.2$, $m_p^1 = 1.6$ $m_c^2 = 38.9$, $m_r^2 = 62.6$, $m_s^2 = 8.8$, $m_p^2 = 2.9$ $m_c^3 = 93.0$, $m_r^3 = 93.5$, $m_s^3 = 24.6$, $m_p^3 = 8.7$
I/r^2 (kg)	$I_c^1 = 18.1$, $I_r^1 = 50.4$, $I_s^1 = 1.7$, $I_p^1 = 1.1$ $I_c^2 = 38.7$, $I_r^2 = 94.2$, $I_s^2 = 3.8$, $I_p^2 = 2.1$ $I_c^3 = 89.8$, $I_r^3 = 145.0$, $I_s^3 = 12.6$, $I_p^3 = 6.8$
Bass Diameter (mm)	$r_c^1 = 91.0$, $r_r^1 = 122.0$, $r_s^1 = 47.0$, $r_p^1 = 37.6$ $r_c^2 = 121.0$, $r_r^2 = 162.0$, $r_s^2 = 63.4$, $r_p^2 = 49.4$ $r_c^3 = 145.0$, $r_r^3 = 203.0$, $r_s^3 = 67.7$, $r_p^3 = 67.7$
Mesh Stiffness (N/m)	$k_{rp}^1 = k_{sp}^1 = 3.8\times10^8$, $k_{rp}^2 = k_{sp}^2 = 5.4\times10^8$, $k_{rp}^3 = k_{sp}^3 = 7.0\times10^8$
Bearing Stiffness (N/m)	$k_c^j = 5.0\times10^8$, $k_r^j = 5.0\times10^8$, $k_s^j = 5.0\times10^8$, $k_p^j = 5.0\times10^8$, j = 1, 2, 3
Torsional Stiffness (N/m)	$k_{cu}^j = 0$, $k_{ru}^j = 1\times10^9$, $k_{su}^j = 0$, j = 1, 2, 3
Coupling Shaft Stiffness (N/m)	$k_{cs}^{ij} = \begin{cases} 1.2\times10^7 & if\ \ i=1,j=2 \\ 2.76\times10^7 & if\ \ i=2,j=3 \\ 0 & otherwise \end{cases}$
Coupling Torsional Stiffness (N/m)	$k_{cs,u}^{ij} = \begin{cases} 1.27\times10^7 & if\ \ i=1,j=2 \\ 2.48\times10^7 & if\ \ i=2,j=3 \\ 0 & otherwise \end{cases}$

3. Modal Properties of Multi-Stage Planetary Gears

To determine the natural frequencies and vibration modes, the time-invariant system is considered. All mesh stiffness are considered to be constant and equal to their average stiffness over one mesh cycle. Thus, the associated eigenvalue problem is

$$\omega^2 M\phi = (K_b + K_m)\phi \tag{5}$$

Where ω is the natural frequency, and ϕ is the vibration modes with the form

$$\phi = [p_c^1, \ldots, p_c^a | p_r^1, \ldots, p_r^a | p_s^1, \ldots, p_s^a | p_p^1, \ldots, p_p^a]^T \tag{6}$$

Where $p_l^j = [x_l^j, y_l^j, u_l^j]^T$, $l = c, r, s$ is for the carriers, rings, and suns, and $p_n^j = [\zeta_n^j, \eta_n^j, u_n^j]^T$, n = 1, 2, …, N^j in p_p^j is for the planet n in the planetary stage j.

In a planetary stage, all planets are assumed equally spaced and have identical model parameters; all bearings have equal stiffness in all

Table 2 Natural frequencies and their multiplicities m for example system

m=1	m=2	
0 R	512.9 P3	155.3 T
277.8 R	890.4 P2	204.6 T
402.7 R	1959.3 P3	227.1 T
460.3 R	2402.4 P3	293.6 T
516.8 R	3010.3 P2	349.8 T
578.7 R	3788.5 P2	406.4 T
673.5 R		485.9 T
888.5 R		585.8 T
963.7 R		648.0 T
1223.0 R		863.8 T
1785.8 R		987.8 T
2344.1 R		1316.2 T
2618.3 R		2140.6 T
3561.1 R		2612.9 T
3901.3 R		3230.8 T
4366.1 R		3676.6 T
5749.0 R		4056.8 T
6488.1 R		4643.6 T

directions; all planets bearing stiffness are equal, all sun-planet mesh stiffness are equal, and all ring-planet mesh stiffness are equal. According to these assumptions, the multi-stage planetary gears become a cyclically symmetric structure. Take the three-stage planetary gear system shown in Fig. 1 as an example. Table 1 lists the main system parameters.[14]

The natural frequencies of the example system are listed in Table 2. Rotational, translational and planet modes are distinguished by R, T, P (P2 for planetary stage 2, P3 for planetary stage 3), respectively. Figs. 4~6 shows the typical vibration modes of each type.

3.1 Rotational modes

The natural frequencies of rotational modes are distinct. All carriers, rings and suns only have rotational motion as shown in Fig. 4. All planets within a planetary stage have the same motion. Thus, a rotation mode has the form:

$$\phi = [p_c^1,\ldots,p_c^a|p_r^1,\ldots,p_r^a|p_s^1,\ldots,p_s^a|p_p^1,\ldots,p_p^a]^T \tag{7}$$

Where $p_l^j=[0,\ 0,\ u_l^j]^T$, $l=c,\ r,\ s,$ and $p_1^j=p_2^j=\ldots=p_{N^j}^j=[\zeta_1^j,\ \eta_1^j,\ u_1^j]^T$, $j=1,\ 2,\ \ldots,\ a$.

3.2 Translational modes

The natural frequencies of translational modes have multiplicity two while all planetary stages have three or more planets. All central gears and carriers only have translational motion as shown in Fig. 5. The pair of degenerated translational modes ($\phi M\bar{\phi}=0$) have the form

$$\begin{cases}\phi = [p_c^1,\ldots,p_c^a|p_r^1,\ldots,p_r^a|p_s^1,\ldots,p_s^a|p_p^1,\ldots,p_p^a]^T\\ \bar{\phi} = [\bar{p}_c^1,\ldots,\bar{p}_c^a|\bar{p}_r^1,\ldots,\bar{p}_r^a|\bar{p}_s^1,\ldots,\bar{p}_s^a|\bar{p}_p^1,\ldots,\bar{p}_p^a]^T\end{cases} \tag{8}$$

Where $p_l^j=[x_l^j,y_l^j,0]^T$, $\bar{p}_l^j=[y_l^j,-x_l^j,0]^T$, $l=c,r,s$ and p_n^j, $\bar{p}_n^j$ in p_p^j, $\bar{p}_p^j$ satisfy

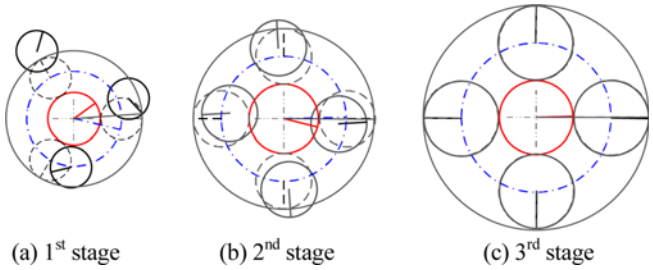

Fig. 4 Typical rotational mode when $\omega_{31}=963.7$ Hz

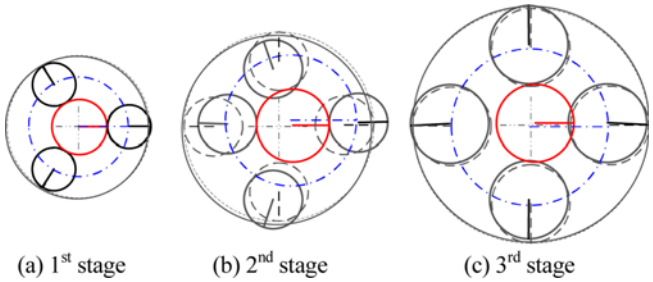

Fig. 5 Typical translational mode when $\omega_{12}=349.8$ Hz

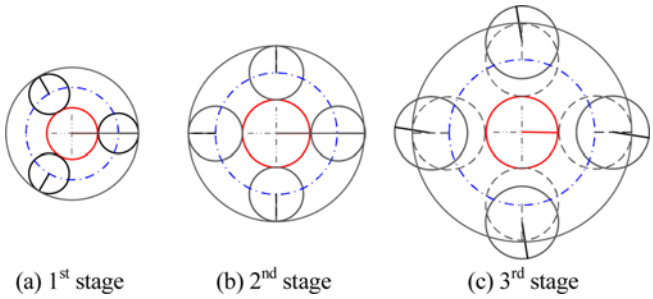

Fig. 6 Typical planet mode when $\omega_{19}=512.9$ Hz

$$\begin{bmatrix}p_n^j\\ \bar{p}_n^j\end{bmatrix}=\begin{bmatrix}I\cos\varphi_n^j & I\sin\varphi_n^j\\ -I\sin\varphi_n^j & I\cos\varphi_n^j\end{bmatrix}\begin{bmatrix}p_1^j\\ \bar{p}_1^j\end{bmatrix} \tag{9}$$

Where $\mathbf{I}$ is an identity matrix, and φ_n^j is the position angle of the planet n in the planetary stage j.

3.3 Planet modes

In planet modes, the natural frequencies have multiplicity N^j-3; the carriers, rings and suns have no motion; only the planets in one planetary stage deflects as shown in Fig. 6. A planet mode has the form

$$\phi = [0,\ldots,0|0,\ldots,0|0,\ldots,0|0,\ldots,p_p^j,0,\ldots 0]^T \tag{10}$$

In addition, the motion of each planet in the planetary stage j is a scalar multiple of any chosen planet in this stage

$$p_p^j=[w_1^j p_1^j, w_2^j p_1^j,\ldots,w_{N^j}^j p_1^j]^T \tag{11}$$

Where the scalar multipliers w_n^j satisfy

Table 3 Expressions of modal strain energies in vibration mode ϕ_i

Modal strain energy
$U_l^{j,v}=\frac{1}{2}k_l^j[(x_l^{j,v})^2+(y_l^{j,v})^2]$
$U_{lu}^{j,v}=\frac{1}{2}k_{lu}^j(u_l^j)^2$
$U_n^{j,v}=\frac{1}{2}k_p^j[(\delta_{cn,x}^{j,v})^2+(\delta_{cn,y}^{j,v})^2]$
$U_{rn}^{j,v}=\frac{1}{2}k_{rp}^j(\delta_{rn}^{j,v})^2$
$U_{sn}^{j,v}=\frac{1}{2}k_{sp}^j(\delta_{sn}^{j,v})^2$
$U_{cs}^{ij,v}=\frac{1}{2}k_{cs,xy}^{ij}[(x_c^{j,v}-x_s^{i,v})^2+(y_c^{j,v}-y_s^{i,v})^2]$
$U_{cs,u}^{ij,v}=\frac{1}{2}\frac{k_{cs,u}^{ij}}{r_c^j}\left(\frac{u_c^{j,v}}{r_c^j}-\frac{u_s^{i,v}}{r_s^i}\right)^2$

$$\sum_{n=1}^{N^j}w_n^j\sin\varphi_n^j=0\,,\ \sum_{n=1}^{N^j}w_n^j\cos\varphi_n^j=0\,,\ \sum_{n=1}^{N^j}w_n^j=0 \tag{12}$$

4. Dominant Vibration Criterion

Considering the typical rotational and translational modes shown in Figs. 4 and 5, a phenomenon can be observed that there is one dominant vibration stage in each mode and component motions of the other stages decrease along the neighboring relation gradually. To analyze the coupling of neighbor stages in multi-stage planetary gears, the dominant vibration criterion of comparing the parameter sensitivities between planetary stages is proposed here.

4.1 Eigensensitivity of multi-stage planetary gears

Using the modal properties discussed above, Parker verified the relations between eigenvalue sensitivities and modal strain energies both in single-stage planetary gears and compound planetary gears.[8,11]

Table 3 shows the expressions of the modal strain energies. The subscripts and superscripts for modal strain energies have the same meanings as for stiffness parameters. For example, $U_l^{j,v}$ means the modal strain energy in the translational bearings stiffness of carrier, ring and sun in planetary stage j.

The relations between eigenvalue sensitivities and modal strain energies can be applied to all three types of vibration modes. The following notation is used: $l=c, r, s$; $i, j=1, 2, \ldots, a$; $n=1, 2, \ldots, N^j$.

Eigenvalue sensitivity to mesh stiffness.

$$\frac{\partial\lambda_v}{\partial k_{sp}^j}=\sum_{n=1}^{N^j}(\delta_{sn}^{j,v})^2=\frac{2}{k_{sp}^j}\sum_{n=1}^{N^j}U_{sn}^{j,v} \tag{13}$$

$$\frac{\partial\lambda_v}{\partial k_{rp}^j}=\sum_{n=1}^{N^j}(\delta_{rn}^{j,v})^2=\frac{2}{k_{rp}^j}\sum_{n=1}^{N^j}U_{rn}^{j,v} \tag{14}$$

Eigenvalue sensitivity to support (bearing) stiffness:

$$\frac{\partial\lambda_v}{\partial k_l^j}=(x_l^{j,v})^2+(y_l^{j,v})^2=\frac{2}{k_l^j}U_{rn}^{j,v} \tag{15}$$

$$\frac{\partial\lambda_v}{\partial k_{lu}^j}=(u_l^{j,v})^2=\frac{2}{k_{lu}^j}U_{lu}^{j,v} \tag{16}$$

$$\frac{\partial\lambda_v}{\partial k_p^j}=\sum_{n=1}^{N^j}[(\delta_{cn,x}^{j,v})^2+(\delta_{cn,y}^{j,v})^2]=\frac{2}{k_p^j}\sum_{n=1}^{N^j}U_n^{j,v} \tag{17}$$

Eigenvalue sensitivity to shaft stiffnesses between carriers and suns in different planetary stages:

$$\frac{\partial\lambda_v}{\partial k_{cs,xy}^{ij}}=(x_c^{j,v}-x_s^{i,v})^2+(y_c^{j,v}-y_s^{i,v})^2=\frac{2}{k_{cs,xy}^{ij}}U_{cs}^{ij,v} \tag{18}$$

$$\frac{\partial\lambda_v}{\partial k_{cs,u}^{ij}}=\left(\frac{u_c^{j,v}}{r_c^j}-\frac{u_s^{i,v}}{r_s^i}\right)^2=\frac{2r_c^j}{k_{cs,xy}^{ij}}U_{cs,u}^{ij,v} \tag{19}$$

4.2 Dominant criterion

In the multi-stage planetary gear system, the total modal strain energy of one planetary stage in mode ϕ_v is

$$\begin{aligned}U^{j,v}=&U_c^{j,v}+U_{cu}^{j,v}+U_r^{j,v}+U_{ru}^{j,v}+U_s^{j,v}+U_{su}^{j,v}\\&+\sum_{n=1}^{N^j}(U_n^{j,v}+U_{rn}^{j,v}+U_{sn}^{j,v})\end{aligned} \tag{20}$$

Where the constituent support or mesh strain energies are related to the parameter sensitivities of vibration modes respectively.

In the model of single-stage planetary gears, Parker showed that particular modes are more or less sensitive to different parameters,[18] and classified the frequencies into two distinct ranges experimentally by comparing the strain energies distribution.[19] Applied to the multi-stage planetary gear system, it is feasible to distinguish the dominant vibration stage by comparing the sensitivities of each mode to the parameters of different stages.

Considering the classification of the vibration modes and their unique properties discussed above, the analysis can be simplified by simplifying the expression of strain energies in multi-stage planetary gears.

Rotational modes: Using the properties of rotational modes shown in Eq. (6), the total modal strain energy of planetary stage j in ϕ_v is reduced to

$$U^{j,v}=U_{cu}^{j,v}+U_{ru}^{j,v}+U_{su}^{j,v}+\sum_{n=1}^{N^j}(U_n^{j,v}+U_{rn}^{j,v}+U_{sn}^{j,v}) \tag{21}$$

Where the six types of strain energy can be related to the sensitivities of vibration modes to different parameters in each planetary stage.

Translational modes: Reducing Eq. (20) using the properties of the traditional modes, the total strain energies in ϕ_v, ϕ_u are respectively:

$$\begin{cases}U^{j,v}=U_c^{j,v}+U_r^{j,v}+U_s^{j,v}+\sum_{n=1}^{N^j}(U_n^{j,v}+U_{rn}^{j,v}+U_{sn}^{j,v})\\U^{j,u}=U_c^{j,u}+U_r^{j,u}+U_s^{j,u}+\sum_{n=1}^{N^j}(U_n^{j,u}+U_{rn}^{j,u}+U_{sn}^{j,u})\end{cases} \tag{22}$$

It can be obviously found that $U_l^{j,v}=U_l^{j,u}$, $l=c, r, s$ using the properties of traditional modes. The translational mode property of Eq. (9) leads to the relations It can be obviously found that $U_l^{j,v}=U_l^{j,u}$, $l=c, r, s$ using the properties of traditional modes. The translational

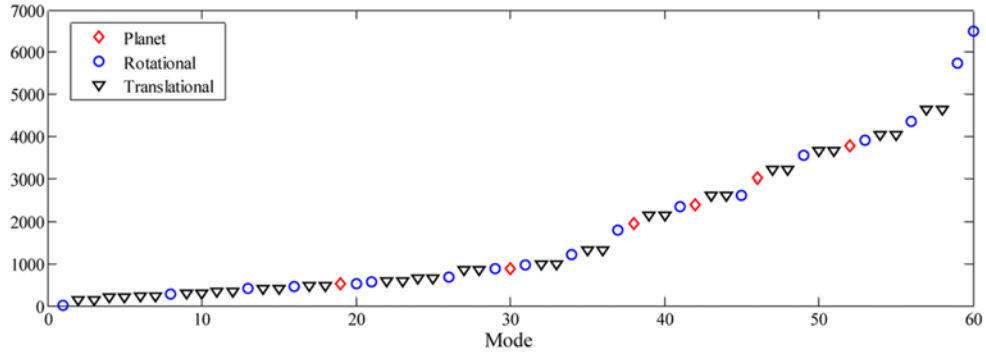

Fig. 7 Natural frequency distributions

mode property of Eq. (9) leads to the relations

$$\begin{bmatrix}\delta_{sn}^{j,u}\\ \delta_{sn}^{j,v}\end{bmatrix}=\begin{bmatrix}\cos\varphi_n^j & \sin\varphi_n^j\\ -\sin\varphi_n^j & \cos\varphi_n^j\end{bmatrix}\begin{bmatrix}\delta_{s1}^{j,u}\\ \delta_{s1}^{j,v}\end{bmatrix} \tag{23}$$

Use of Eq. (23) in the expression of strain energies shown in Table 3 yields

$$\sum_{n=1}^{N^j}U_{sn}^{j,u}=\sum_{n=1}^{N^j}U_{sn}^{j,v}=\frac{1}{2}k_{sp}^j[(\delta_{s1}^{j,v})^2+(\delta_{s1}^{j,u})^2] \tag{24}$$

With the same analysis method, the follow equations can be derived too

$$\sum_{n=1}^{N^j}U_{n}^{j,u}=\sum_{n=1}^{N^j}U_{n}^{j,v},\ \sum_{n=1}^{N^j}U_{rn}^{j,u}=\sum_{n=1}^{N^j}U_{rn}^{j,v} \tag{25}$$

Therefore, the total modal strain energies of two degenerate modes ϕ_v, ϕ_u are identical. It is just needed to analyze one of them.

Planet mode: Using the properties of planet modes, only one planetary stage has component deflections in planet modes, which can be considered as the dominant vibration stage logically.

5. Application

The multi-stage planetary gears in a TBM driving train shown in Fig. 1 is used as an example. The modal parameters are given in Table 1. Table 2 shows the analytical natural frequencies with identified mode type. The natural frequency distributions are shown in Fig. 7, where the modes have been classified into rotational, translational and planet modes according to previous studies. However, this classification only reveals the information about central member motion in general. Because of the multiple degrees of freedom in multi-stage planetary gear system, which is identified to the number of natural frequencies and vibration modes, it is imperative to study more detailed classification of vibration modes by analyzing mode characteristics.

5.1 Distinguishing dominant vibration stage

Fig. 8 illustrates the parameter sensitivity distributions of each rotational, translational modes, and planet modes, where x coordinate is the natural frequencies associated with vibration modes, y coordinate enumerates the types of parameter sensitivity in each mode type discussed above, and z coordinate means the sensitivity value.

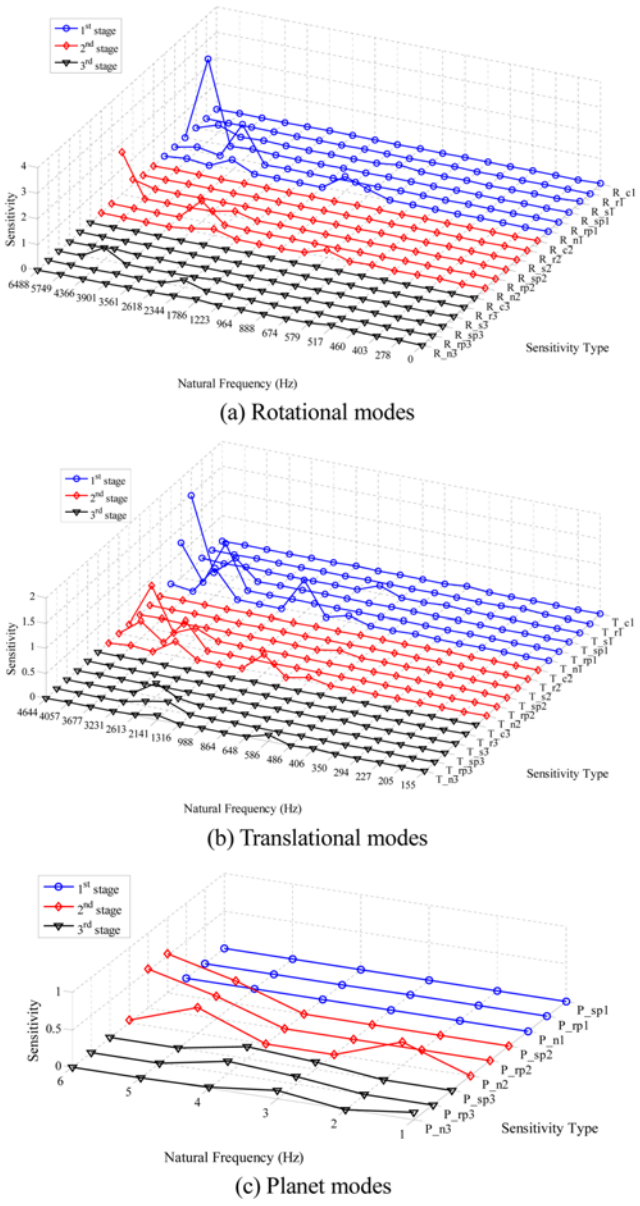

Fig. 8 Comparison of parameter sensitivity distributions among the vibration modes

Comparing the parameter sensitivities among all the vibration modes,

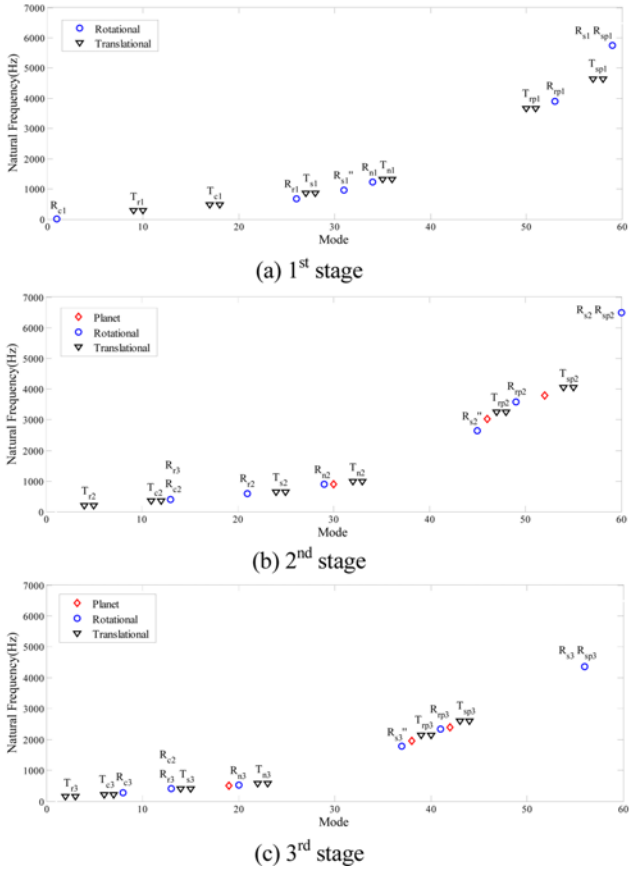

Fig. 9 Natural frequencies classified by the dominant vibration stage

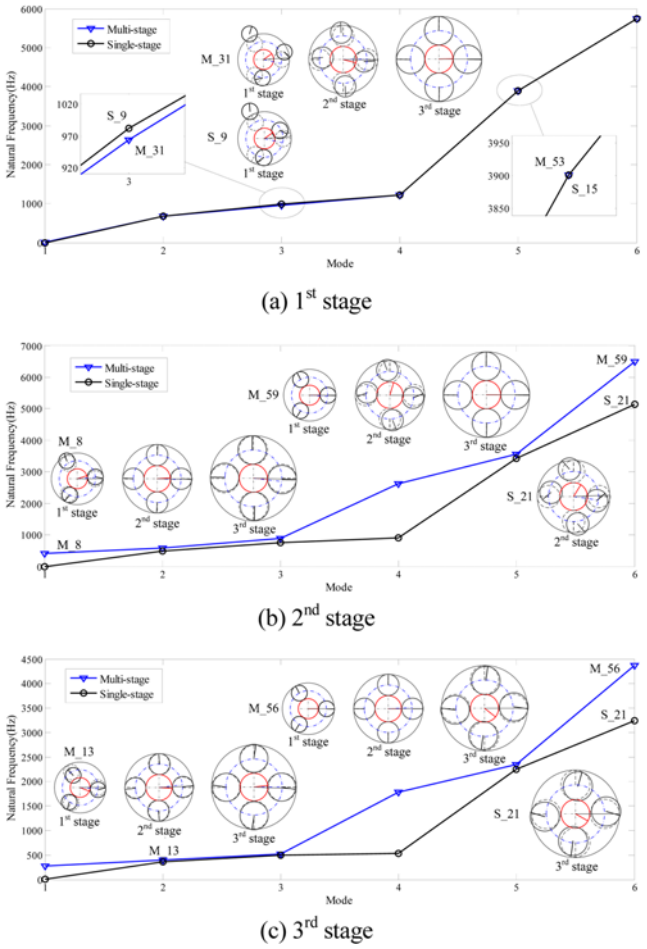

Fig. 10 Comparison of the rotational modes between single and multi-stage planetary gear system

the dominant vibration stages are distinguished. Then, collecting these results of vibration modes with distinguished dominant vibration stage in the rotational and translational mode types, and gathering the calculated planet modes in Table 2, the natural frequencies are presented as three associated stages shown in Fig. 9.

5.1.1 Rotational modes

In Fig. 6, "R_{s1}" means the rotational frequency with the highest sensitivity of k_s^1 (the torsional stiffness of the sun in the first stage of the example system), and "R_{s1}" means the second highest sensitivity. The parameter sensitivities of k_{sp}^j, k_{rp}^j and k_p^j (the bearing stiffness of the planets and the mesh stiffness of the sun-planet and ring-planet meshes in each stage of the example system) reach the highest at the last three frequencies in each figure of Fig. 9, respectively. In contrast, k_c^j and k_r^j occur at the first two frequencies, while the highest sensitivities of k_c^2 and k_r^3 both occur at the same frequencies. The maximum values of k_{sp}^j and k_s^j occur at the same rotational frequencies concurrently, too. However, the second maximum values of k_s^j distribute at different frequencies. Finally, at the end of the above analysis, the frequency ω_{16} is associated to no highest sensitivity, so it does not exist in Fig. 9.

5.1.2 Translational modes

There is a good property for translational modes; the maximum value of all the parameter sensitivities exactly occurs at different pairs of translational frequencies. Therefore, the associated stage of translational modes can be classified clearly, and each stage has the similar pairs shown in Fig. 9, where "T_{r3}" means the translational frequency with the highest sensitivity of the bearing stiffness of ring in the third stage of the example system. In addition, there are two frequency bands defined by the parameter sensitivity distributions and component deflections in the mode. The first three pairs of translational modes in each figure correspond to the maximum value of parameter sensitivity to the bearing stiffness of carrier, ring and sun, respectively. In contrast, the last three pairs respectively associate with the highest parameter sensitivity to the bearing stiffness of the planets and the mesh stiffness of the sun-planet mesh, ring-planet mesh.

5.1.3 Planet modes

In Fig. 9(b) and 9(c), the planet modes are only found in the right half range, where the rotational and translational frequencies with the highest parameter sensitivities of k_{sp}^j, k_{rp}^j and k_p^j exist in the same range.

5.2 Comparison of frequencies and vibration modes with single-stage planetary gears

Consider the natural frequencies and vibration modes in the three single-stage planetary gear systems, which consist of the example system shown in Fig. 1 and Table 1. Then compare them with the frequencies

and vibration modes of the example system, which are classified by the dominant vibration stage shown in Fig. 9.

5.2.1 Rotational modes

Fig. 10 shows the comparison of the rotational modes. In Fig. 10(a), there are more component amplitude in the first stage of the vibration modes of the multi-stage planetary gear system, and they are similar to the modes in the single-stage planetary gear system, which has the same parameters of the first stage in the example system shown in Table 1. Meanwhile, the frequencies of these two planetary gear systems are approximate; however, enlarging the zoom, the frequency gaps between them are reduced as the frequency value increases.

Fig. 10(b) and 10(c) show the comparison associated with the second and the third stage. Different from the first stage, the frequencies in the multi-stage planetary gear system are smaller than those in the single planetary gear systems, and the frequency gaps are widened as the frequency increases. However, comparing the modes of the dominant vibration stage in the multi-stage planetary gear system with the modes of single-stage planetary gear system shown in Fig. 10(b) and 10(c), it is found that the components are approximate in the higher frequency range, but different in the lower frequency range.

There is one duplicate frequency (ω_{13}) in Fig. 10(b) and 10(c), which means the maximum sensitivities of k_c^2 and k_r^3 occur at the same rotational frequency. Checking the mode of this duplicate frequency shown in Fig. 10(c), the amplitudes of the planet motions in all the three stages are closed, and it is difficult to distinguish which the dominant vibration stage is.

As analyzed in the section 5.1.1, there is an omitted rotational frequency (ω_{16}) which does not exist in Figs. 9 and 6. The associated modes are shown in Fig. 11. Similar to the mode of the duplicate frequency in Fig. 10, components of all the three stages deflect, and the component deflections in each stage are approximate. By coincidence, both the tow frequencies are landing in the lower frequency range. It can be explained that the coupling of each stage in the rotational modes of the multi-stage planetary gear system grows as the frequency reduces.

5.2.2 Translational modes

Fig. 9 shows the comparison of the translational modes. Similar to the property analyzed in the rotational modes associated to the first stage shown in Fig. 10(a), there are more component amplitude in the distinguished dominant vibration stage. Comparing the component deflections of the dominant stage with the modes of independent single-stage planetary gears shown in Fig. 12, they are similar too. Meanwhile, the frequencies of these two planetary gear systems are approximate, enlarging the zoom, the frequency gaps between them reduce as the frequency value increase. It can be summarized that the coupling of each stage in the rotational modes of the multi-stage planetary gear system grows as the frequency reduces too.

5.2.3 Planet modes

For concision, take the third stage as example, Fig. 13 shows the comparison of the planet modes between the multi-stage planetary gear system shown Table 1 and the single-stage planetary gear system with the same parameters of the third stage. The frequencies in each type of planetary gear system are identical, as well as the vibration modes.

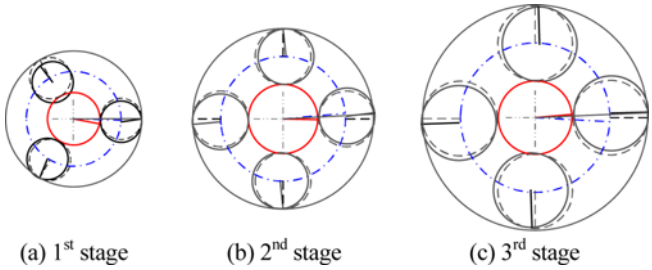

Fig. 11 The omitted rotational modes when $\omega_{16} = 460.3$ Hz

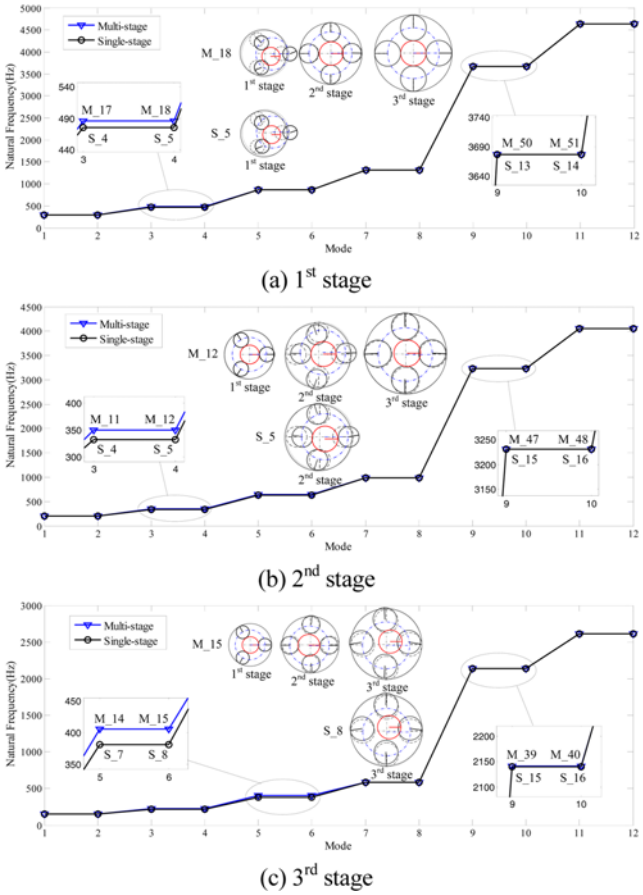

Fig. 12 Comparison of the translational modes between single and multi-stage planetary gear system

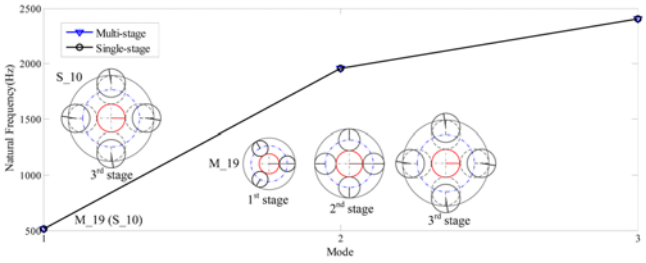

Fig. 13 Comparison of the planet modes between single and multi-stage planetary gear system

Overall, the dominant vibration stage of each natural frequencies in

the example multi-stage planetary gears are distinguished, and the eigensensitivity distributions to different component parameters are proposed. These results are useful in the experimental study of modal properties of multi-stage planetary gears. For example, the high-frequency are shown high sensitivity to planet mesh stiffnesses, in other words, high-frequency modes contains high strain energy in the planet meshes, which determines that a component of planetary gear must be excited directly to adequately excite all the high-frequency modes in the modal tests.

6. Conclusions

(1) A dynamic model of multi-stage planetary gears of general description has been developed. The vibration modes of the multi-stage planetary gears with identical, equally spaced planets can be classified into rotational, translational and planet modes. In each rotational and translational modes, coupling between planetary stages is observed, and there is one dominant vibration stage with significant component deflections. Only one planetary stage of planets exists as motions in planet modes.

(2) Each translational mode can be marked by one different highest parameter sensitivity. Mesh stiffness and planet bearing stiffness of each stage are associated with the higher frequencies, while bearing stiffness of carriers, rings, and suns are associated with the lower frequencies. In rotational modes, the highest eigensensitivity to mesh stiffness and planets bearing stiffness of each stage occurred at different higher frequencies. For lower rotational frequencies, the highest eigensensitivity to bearing stiffness of carriers, rings in different planetary stages may occur at the same modes.

(3) The modal properties of multi-stage planetary system are similar to the single-stage planetary gear system with the same parameters of dominant vibration stage. For translational modes, the component motions of dominant vibration stage are similar to the modes of single-stage planetary gear system, and the natural frequencies of two systems are approximate, especially for the higher frequencies. For planet modes, both the natural frequencies and vibration modes are similar to the single-stage planetary gear system. For rotational modes, only the component motions of dominant vibration stage in higher frequency range are similar to the modes of single-stage planetary gear system, but the frequency gap between two systems increase as the frequency grows up. In general, the coupling of neighbor stages in the multi-stage planetary gear system grows as the frequency reduces.

(4) The analytical method proposed in this paper can clearly identify the frequencies and vibration modes of multi-stage planetary stage system, which provides effective support for studying the dynamics of multi-stage planetary gear system.

ACKNOWLEDGMENT

The authors would like to acknowledge the support and contributions from the School of Mechanical Engineering, Dalian University of Technology, China. The research is supported by National Basic Research Program of China (973 Program, Grant No. 2013CB035402).

REFERENCES

1. Smith, J. K., "Gear Noise and Vibration," Marcel Dekker, pp. 201-205, 2003.
2. Kahraman, A., "Free Torsional Vibration Characteristics of Compound Planetary Gear Sets," Mechanism and Machine Theory, Vol. 36, No. 8, pp. 953-971, 2001.
3. Lin, J. and Parker, R. G., "Analytical Characterization of the Unique Properties of Planetary Gear Free Vibration," Journal of Vibration and Acoustics, Vol. 121, No. 3, pp. 316-321, 1999.
4. Ericson, T. M. and Parker, R. G., "Natural Frequency Clusters in Planetary Gear Vibration," Journal of Vibration and Acoustics, Vol. 135, No. 6, Paper No. 061002, 2013.
5. Eritenel, T. and Parker, R. G., "Modal Properties of Three-Dimensional Helical Planetary Gears," Journal of Sound and Vibration, Vol. 325, No. 1, pp. 397-420, 2009.
6. Wu, S., Liu, Z., Wang, X., and Zhu, E., "Nonlinear Dynamic Characteristics of Compound Planetary Gear Train Sets based on Harmonic Balance Method," Jixie Gongcheng Xuebao(Chinese Journal of Mechanical Engineering), Vol. 47, No. 1, pp. 55-61, 2011.
7. Abousleiman, V., Velex, P., and Becquerelle, S., "Modeling of Spur and Helical Gear Planetary Drives with Flexible Ring Gears and Planet Carriers," Journal of Mechanical Design, Vol. 129, No. 1, pp. 95-106, 2007.
8. Lin, J. and Parker, R. G., "Sensitivity of Planetary Gear Natural Frequencies and Vibration Modes to Model Parameters," Journal of Sound and Vibration, Vol. 228, No. 1, pp. 109-128, 1999.
9. Wang, S. Y., Song, Y. M., Shen, Z. G., Zhang, C., Yang, T. Q., and Xu, W. D., "Research on Natural Characteristics and Loci Veering of Planetary Gear Transmissions," Journal of Vibration Engineering, Vol. 18, No. 4, pp. 412-417, 2005.
10. Kiracofe, D. R. and Parker, R. G., "Structured Vibration Modes of General Compound Planetary Gear Systems," Journal of Vibration and Acoustics, Vol. 129, No. 1, pp. 1-16, 2007.
11. Guo, Y. and Parker, R. G., "Sensitivity of General Compound Planetary Gear Natural Frequencies and Vibration Modes to Model Parameters," Journal of Vibration and Acoustics, Vol. 132, No. 1, Paper No. 011006, 2010.
12. Qin, D. T., Xing, Z. K., and Wang, J. H., "Optimization Design of System Parameters of the Gear Transmission of Wind Turbine based on Dynamics and Reliability," Chinese Journal of Mechanical Engineering, Vol. 44, No. 7, pp. 24-31, 2008.
13. Wei, J., Sun, Q., Sun, W., Ding, X., Tu, W., and Wang, Q., "Load-Sharing Characteristic of Multiple Pinions Driving in Tunneling Boring Machine," Chinese Journal of Mechanical Engineering, Vol. 26, No. 3, pp. 532-540, 2013.
14. Qin, D., Xiao, Z., and Wang, J., "Dynamic Characteristics of Multi-Stage Planetary Gears of Shield Tunnelling Machine based on Planet

Mesh Phasing Analysis," Jixie Gongcheng Xuebao (Chinese Journal of Mechanical Engineering), Vol. 47, No. 23, pp. 20-29, 2011.

15. Wei, J., Lv, C., Sun, W., Li, X., and Wang, Y., "A Study on Optimum Design Method of Gear Transmission System for Wind Turbine," Int. J. Precis. Eng. Manuf., Vol. 14, No. 5, pp. 767-778, 2013.
16. Kahraman, A., "Planetary Gear Train Dynamics," Journal of Mechanical Design, Vol. 116, No. 3, pp. 713-720, 1994.
17. Jing, W., Cheng, L., Wei, S., and Jin, C., "Study on the Mode Characteristics and Parameter Sensitivity for NGW Planetary Gear System," Journal of Vibration Engineering, Vol. 26, No. 5, pp. 654-664, 2013.
18. Lin, J. and Parker, R. G., "Natural Frequency Veering in Planetary Gears," Mechanics of Structures and Machines, Vol. 29, No. 4, pp. 411-429, 2001.
19. Lin, J. and Parker, R. G., "Natural Frequency Veering in Planetary Gears," Mechanics of Structures and Machines, Vol. 29, No. 4, pp. 411-429, 2001.